# The ladder-shaped polyether toxin gambierol anchors the gating machinery of Kv3.1 channels in the resting state

Ivan Kopljar,[1] Alain J. Labro,[1] Tessa de Block,[1] Jon D. Rainier,[2] Jan Tytgat,[3] and Dirk J. Snyders[1]

[1]Laboratory for Molecular Biophysics, Physiology and Pharmacology, University of Antwerp, 2610 Antwerp, Belgium
[2]Department of Chemistry, University of Utah, Salt Lake City, UT 84112
[3]Laboratory for Toxicology, Campus Gasthuisberg, University of Leuven, 3000 Leuven, Belgium

Voltage-gated potassium (Kv) and sodium (Nav) channels are key determinants of cellular excitability and serve as targets of neurotoxins. Most marine ciguatoxins potentiate Nav channels and cause ciguatera seafood poisoning. Several ciguatoxins have also been shown to affect Kv channels, and we showed previously that the ladder-shaped polyether toxin gambierol is a potent Kv channel inhibitor. Most likely, gambierol acts via a lipid-exposed binding site, located outside the $K^+$ permeation pathway. However, the mechanism by which gambierol inhibits Kv channels remained unknown. Using gating and ionic current analysis to investigate how gambierol affected S6 gate opening and voltage-sensing domain (VSD) movements, we show that the resting (closed) channel conformation forms the high-affinity state for gambierol. The voltage dependence of activation was shifted by >120 mV in the depolarizing direction, precluding channel opening in the physiological voltage range. The (early) transitions between the resting and the open state were monitored with gating currents, and provided evidence that strong depolarizations allowed VSD movement up to the activated-not-open state. However, for transition to the fully open (ion-conducting) state, the toxin first needed to dissociate. These dissociation kinetics were markedly accelerated in the activated-not-open state, presumably because this state displayed a much lower affinity for gambierol. A tetrameric concatemer with only one high-affinity binding site still displayed high toxin sensitivity, suggesting that interaction with a single binding site prevented the concerted step required for channel opening. We propose a mechanism whereby gambierol anchors the channel's gating machinery in the resting state, requiring more work from the VSD to open the channel. This mechanism is quite different from the action of classical gating modifier peptides (e.g., hanatoxin). Therefore, polyether toxins open new opportunities in structure–function relationship studies in Kv channels and in drug design to modulate channel function.

The Journal of General Physiology

## INTRODUCTION

Gambierol is a ladder-shaped polyether toxin from the ciguatoxin-producing dinoflagellate *Gambierdiscus toxicus* (Satake et al., 1993). Ciguatoxins are well known modulators of voltage-gated sodium (Nav) channels and cause ciguatera food poisoning (Nicholson and Lewis, 2006). These toxins enhance cellular excitability by shifting the threshold for Nav channel opening toward more negative potentials and/or by destabilizing the inactivation process (Catterall et al., 2007). Several ciguatoxins have been identified as potent voltage-dependent potassium (Kv) channel inhibitors as well, suggesting a potential contribution of Kv channel inhibition to ciguatera (Hidalgo et al., 2002; Birinyi-Strachan et al., 2005; Mattei et al., 2010; Schlumberger et al., 2010a,b). Gambierol does not affect Nav channel function (Ghiaroni et al., 2005; Cuypers et al., 2008), but inhibits Kv1 and Kv3 subtypes in the nanomolar range (Cuypers et al., 2008; Kopljar et al., 2009).

Kv channels are tetramers of α subunits, each with a six-transmembrane segment (S1–S6) topology. The S5–S6 segments coassemble with a fourfold symmetry into the central $K^+$ permeation pore that is surrounded by four voltage-sensing domains (VSDs) composed of S1–S4 (Long et al., 2005). Opening of Kv channels requires that the VSD of each subunit moves from the resting to the activated state; when all four subunits have reached this activated-not-open state, gate opening proceeds in a "concerted" manner (Bezanilla et al., 1994; Zagotta et al., 1994b; Schoppa and Sigworth, 1998; Ledwell and Aldrich, 1999). At the molecular level, the outward movement (activation) of the VSD transduces via an electromechanical coupling to the activation gate in the bottom part of the S6 segment (S6 gate; Lu et al., 2002; Long et al., 2005; Blunck and Batulan, 2012; Labro and Snyders, 2012). Conversely, the inward movement of the VSD toward its resting state closes the S6 gate. We showed previously that the molecular determinants for inhibition of Kv3.1 by gambierol are located outside the $K^+$ pore and involve lipid-facing residues on

Correspondence to Dirk J. Snyders: dirk.snyders@ua.ac.be
Abbreviation used in this paper: VSD, voltage-sensing domain.



The Rockefeller University Press $30.00
J. Gen. Physiol. Vol. 141 No. 3 359–369
www.jgp.org/cgi/doi/10.1085/jgp.201210890

both the S5 and S6 segment of the α subunits (Kopljar et al., 2009). This high-affinity binding site is accessible in the closed state, and, in contrast to gating modifiers such as hanatoxin (Swartz, 2007), short depolarizations did not overcome the inhibition.

To address the mechanism by which gambierol inhibits its Kv channels, we used gating and ionic current analysis to track the VSD movement and the S6 gate opening, respectively. By examining the state-dependent inhibition of Kv3.1 gating and ionic currents, and by controlling the number of high-affinity binding sites using tetrameric concatemers, we show that gambierol binds with high affinity to the resting (closed) state of the channel. When bound, the voltage dependence of activation is shifted by >120 mV toward more depolarized potentials, as if gambierol anchors the gating machinery in the resting state. This condition can be reversed by very strong depolarizations that push the subunits toward the low-affinity activated state from which channel opening proceeds upon gambierol unbinding. These findings represent a novel mechanism of gating modification in Kv channels by a ladder-shaped polyether toxin where the resting state is the high-affinity site and binding of gambierol to a single binding site is sufficient to inhibit ion permeation.

## MATERIALS AND METHODS

### Molecular biology

Kv3.1b was cloned in a pEGFP-N1 expression vector. Concatemeric constructs were created using the QuikChange Site-Directed Mutagenesis kit (Agilent Technologies) and mutant primers. Each monomer was tagged with a linker sequence of 60 bp containing a unique restriction-enzyme digest site that was used to link the monomers together. Double strand sequencing using the EZ-Tn5 <TET-1> Insertion kit (Epicentre) confirmed the presence of the desired modifications and the absence of unwanted mutations. Plasmid DNA was amplified in XL2 blue script cells (Agilent Technologies) and isolated using the GenElute HP plasmid maxiprep kit (Sigma-Aldrich).

### Electrophysiology

$Ltk^-$ cells (mouse fibroblasts, ATCC CLL.1.3) were cultured in Dulbecco's modified Eagle's medium with 10% horse serum and 1% penicillin/streptomycin. Cells were transiently transfected with 50–250 ng plasmid DNA for monomer or concatemer constructs using polyethyleneimine (PEI; Sigma-Aldrich); for gating current measurements, 5 µg of plasmid DNA was transfected.

20 h (48 h for gating currents) after transfection, ionic and gating current measurements were done at room temperature (20–23°C) with an Axopatch-200B amplifier, and the recordings were digitized with a Digidata-1200A (Axon Instruments). Command voltages and data storage were controlled with pClamp8 software. Patch pipettes were pulled from 1.2-mm quick-fill borosilicate glass capillaries (World Precision Instruments) with a P-2000 puller (Sutter Instrument Co.) and heat polished afterward. The bath solution contained (in mM) 130 NaCl, 4 KCl, 1.8 $CaCl_2$, 1 $MgCl_2$, 10 Hepes, and 10 glucose, adjusted to pH 7.35 with NaOH. The pipette solution contained (in mM) 110 KCl, 5 $K_4$BAPTA, 5 $K_2$ATP, 1 $MgCl_2$, and 10 Hepes, adjusted to pH 7.2 with KOH. Junction potentials were zeroed with the filled pipette in the bath solution. Experiments were excluded from analysis if the voltage error estimate exceeded 5 mV after series resistance compensation.

Kv3.1 gating currents were recorded in the whole-cell configuration by replacing monovalent cations with TEA in the external solution and with $NMG^+$ in the internal solution. For gating current measurements, the bath solution contained (in mM) 140 TEA-Cl, 10 Hepes, 10 glucose, 1 $MgCl_2$, and 1.8 $CaCl_2$, adjusted to pH 7.35 with TEA-OH. The pipette solution contained (in mM) 140 $NMG^+$, 10 Hepes, 10 EGTA, and 1 $MgCl_2$, adjusted to pH 7.2 with HCl. After compensation, the remaining capacitive transients were subtracted using a −P/8 protocol.

Gambierol (CAS 146763–62-4) was synthesized as described previously (Johnson et al., 2006). Because of its lipophilic character, stock solutions were prepared as 20 µM and 300 µM in DMSO and diluted with the external solution to appropriate concentrations. The final DMSO concentration never exceeded 0.5% and toxins were applied using a fast perfusion system (ALA Scientific Instruments).

### Data analysis

Dose–response curves were obtained by plotting $y$, the fraction of current remaining, as a function of toxin concentration $T$ and fitted with the Hill equation $1 - y = 1/\{1 + (IC_{50}/[T])^{nH}\}$, where $IC_{50}$ is the concentration that generates 50% inhibition and $n_H$ is the Hill coefficient. The voltage dependence of activation and inactivation was fitted with a single Boltzmann equation. Time constants were determined by fitting the current recordings with a single exponential function. Charge (Q) measurements were obtained by integrating the $I_{gOFF}$ and/or $I_{gON}$ currents over sufficient time. The time constants of $I_{gOFF}$ and $I_{gON}$ decay were determined with a single or double exponential function. Results are expressed as mean ± SEM, with $n$ being the number of cells analyzed; error bars are shown if larger than symbol size.

To express the shift in the voltage dependence of gating charge activation in terms of free energy difference between the resting and the activated state, we calculated the Gibbs free energy of gating current activation at 0 mV ($\Delta G_0$) for control condition and in the presence of gambierol. Fitting the charge (Q) versus voltage (V) QV curves with a Boltzmann function yielded a midpoint potential $V_{1/2}$ and a slope factor k = RT/zF, with z as the equivalent charge, and F, R, and T having their usual meaning. $\Delta G_0$ was then calculated as $0.2389 \times zFV_{1/2}$, with the factor 0.2389 to express the values in Kcal/mol (Li-Smerin et al., 2000).

### Online supplemental material

Fig. S1 shows the design of concatemers, their Western Blot analysis, and their biophysical properties. Fig. S2 shows the washout of gambierol for the low-affinity T427V mutant, indicating that any lipid (de)partitioning of gambierol out of the membrane is not the rate-limiting step in the overall process of toxin–channel interaction. Online supplemental material is available at http://www.jgp.org/cgi/content/full/jgp.201210890/DC1.

## RESULTS

### Kv3.1 channels display a state-dependent affinity for gambierol

Previously, we proposed that the ladder-shaped polyether toxin gambierol is a gating modifier that acts at the lipid-exposed surface of the pore domain and stabilizes the closed pore conformation through a yet-unresolved mechanism (Kopljar et al., 2009). Inhibition by gambierol did not require channel opening (Kopljar

et al., 2009), but to explore whether gambierol can also inhibit channels in the open conformation, 100 nM gambierol was applied during a prolonged membrane depolarization to +60 mV (a potential where most channels quickly reach the open conformation). If inhibition would be state-independent, there should be ~37% reduction in total current 30 s after gambierol application because the time constant of inhibition for 100 nM gambierol was ~65 s (Kopljar et al., 2009). Fig. 1 A shows that after the 30-s test pulse, there was no marked difference in the currents between control conditions and after gambierol application. This indicated that gambierol cannot exert its potent inhibiting effect at depolarized potentials, i.e., on open or inactivated channels. Interestingly, the time constant for induction of subsequent inhibition (monitored by 250-ms steps to +40 mV every 10 s) was 36 ± 3 s ($n = 4$; Fig. 1 B), which is approximately twice as fast compared with the onset (time constant of 65 s) obtained by monitoring current inhibition upon fast application of gambierol (Kopljar et al., 2009). This difference might reflect the establishment of a steady-state gambierol concentration in the vicinity of the channel's binding site, i.e., a lipid partitioning step.

If the open state of Kv3.1 channels has a lower affinity for gambierol, then established inhibition in the closed state might be relieved by pushing the bound channels to the open conformation. However, unlike hanatoxin (Swartz and MacKinnon, 1997), we could not detect activation of ionic current with short steps (Kopljar et al., 2009); therefore, we applied prolonged and strong depolarizations (up to +140 mV) in the presence of gambierol. Indeed, steps to potentials >+80 mV induced significant current recovery (Fig. 1, C and D), which amounted to 29.2 ± 5.8% ($n = 4$) after 5 s at +140 mV (Fig. 1 E). Furthermore, the reinhibition of the recovered current was not instantaneous but proceeded with a time constant of 39 ± 5 s ($n = 4$), which suggests that the ionic current recovery was caused by unbinding of gambierol.

### Characterization of Kv3.1 gating currents

Kv channels can detect changes in the membrane potential by their positively charged VSDs, which rearrange and result in a transient charge displacement detectable as a gating current (Bezanilla, 2008). Because of the fourfold symmetry, each Kv channel possesses four identical VSDs, which all need to move from their resting (inward-facing) "down" state to their active (outward-facing) "up" state before the concerted step can occur that leads to S6 gate opening and ion permeation (Zagotta et al., 1994a; Schoppa and Sigworth, 1998).

The voltage dependence of gating charge movement in Kv3.1 channels was determined using a classical activation voltage protocol (Fig. 2, A and B). Integrating

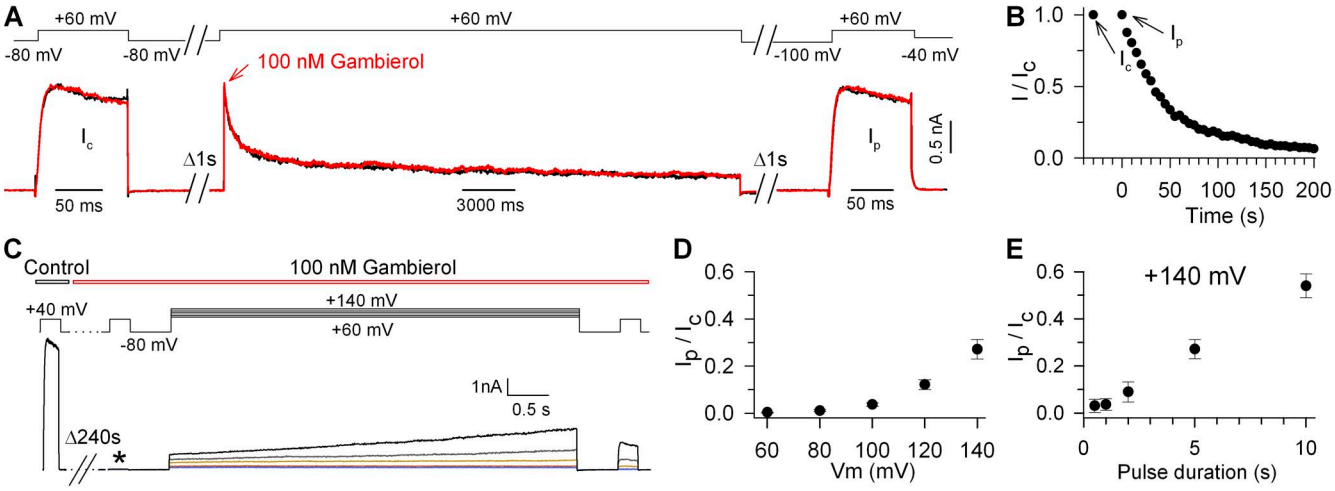


**Figure 1.** State-dependent inhibition of Kv3.1. (A) The potential inhibition of the open state for gambierol was tested by applying 100 nM gambierol during a 30-s depolarizing pulse to +60 mV. The corresponding currents are shown in the absence (black) or presence (red) of gambierol. After a control 100-ms prepulse ($I_c$) to +60 mV, gambierol was added simultaneously with the start of the subsequent 30-s depolarization (arrow). Thereafter, the membrane was clamped to −100 mV for 2 s to recover all inactivated channels, followed by a step to +60 mV to determine the postpulse amplitude ($I_p$). The ratio of $I_p/I_c$ was 98.5 ± 0.6% ($n = 4$) in control and 98.7 ± 1.1% ($n = 4$) with gambierol, indicating that there was no gambierol inhibition during the 30-s long depolarization. (B) Subsequent establishment of inhibition at −80 mV after the 30-s step shown in A. (C) Slow recovery from inhibition by strong depolarizations. After a control 100-ms step to +40 mV ($I_c$), full inhibition was established with 100 nM gambierol, as confirmed by the lack of current at +40 mV recorded 240 s after gambierol wash-in (asterisk). In the continued presence of gambierol, 5-s depolarizing steps to potentials between +60 and +140 mV were applied. The recovered ionic current was quantified with a postpulse step to +40 mV ($I_p$). (D) Fractional current recovery ($I_p/I_c$) as a function of the step potential in C. (E) Time dependence of current recovery at +140 mV from fractional current recovery as a function of the pulse duration. Error bars indicate SEM.

either ON currents ($I_{gON}$) or OFF currents ($I_{gOFF}$) and plotting them as a function of the depolarizing potential yielded similar QV curves, displaying a midpoint potential ($V_{1/2}$) of 7.2 ± 1.8 mV with slope factor ($k$) of 7.2 ± 1.2 mV for $I_{gON}$ ($n$ = 4) and a $V_{1/2}$ of 5.8 ± 1.9 mV with a $k$ of 6.5 ± 0.3 mV for $I_{gOFF}$ ($n$ = 7), respectively. These data are in agreement with previous gating current studies of Kv3.1 channels (Shieh et al., 1997). Compared with the voltage dependence of channel opening with a $V_{1/2}$ of 23.5 ± 1.0 mV and a $k$ of 5.6 ± 0.3 mV ($n$ = 5), the QV curve was shifted ~15 mV toward more hyperpolarized potentials, similar to observations in other *Shaker*-type Kv channels (Perozo et al., 1992). Another well-conserved characteristic of the gating charge movement in Kv channels is a time- and voltage-dependent slowing of the $I_{gOFF}$ decay upon channel gate opening (Stefani et al., 1994; Wang et al., 2007). This slowing in $I_{gOFF}$ kinetics provides direct information on whether or not the final concerted step leading to S6 gate opening has been passed. Therefore, we characterized the slowing in $I_{gOFF}$ decay of Kv3.1 channels using an envelope protocol with steps of different durations to +60 mV and −5 mV, respectively (Fig. 2 D). Very short depolarizations to +60 mV generated an $I_{gOFF}$ that decayed mono-exponentially with a time component $\tau_{OFF,fast}$ of 0.35 ± 0.02 ms ($n$ = 6) at −80 mV, whereas after prolonged depolarizations $I_{gOFF}$ decayed markedly slower, with a $\tau_{OFF,slow}$ of 3.44 ± 0.11 ms ($n$ = 6). Intermediate step durations resulted in bi-exponential $I_{gOFF}$ decays that were a weighted combination of both the fast ($I_{gOFF,fast}$) and the slow ($I_{gOFF,slow}$) component. In contrast, depolarizations to −5 mV, which is below the apparent threshold for channel opening, resulted in fast mono-exponential decaying $I_{gOFF}$, with a $\tau_{OFF,fast}$ of 0.20 ± 0.02 ms ($n$ = 3), irrespective of the duration of depolarization.

4-Aminopyridine (4-AP) is a universal Kv channel inhibitor (Grissmer et al., 1994) and has been shown to inhibit *Shaker* Kv channels by preventing the channels from passing the concerted step leading to S6 gate

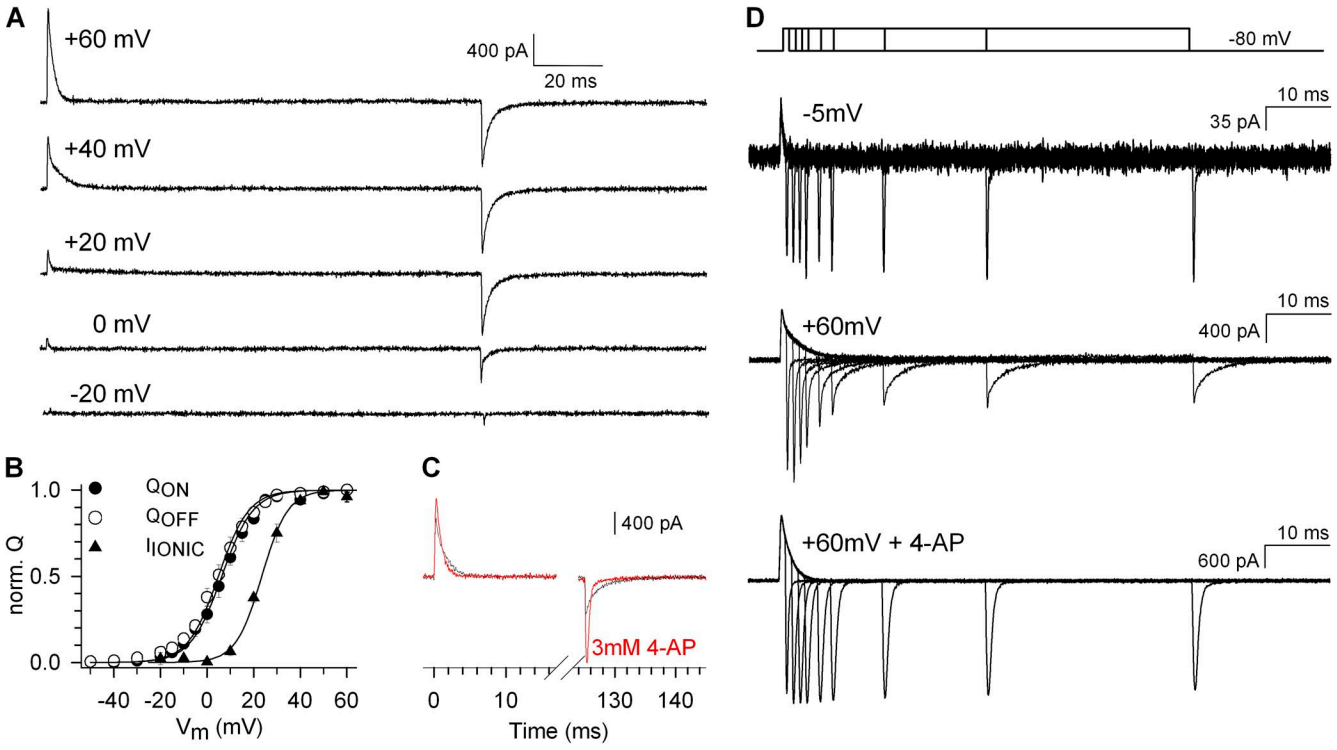


**Figure 2.** Properties of Kv3.1 gating currents. (A) Gating currents elicited by 125-ms steps from −80 mV to various depolarizing potentials ($I_{gON}$), followed by a return of the charge ($I_{gOFF}$) during repolarization back to −80 mV. (B) Normalized QV relationships for $I_{gON}$ and $I_{gOFF}$ fitted with a single Boltzmann function (solid lines). The voltage dependence of channel opening is shown with triangles. (C) Effect of 4-AP on gating currents. In control, $I_{gOFF}$ showed a bi-exponential decay with fast and slow time constants of 0.69 ± 0.07 ms and 3.39 ± 0.18 ms ($n$ = 5), respectively. Application of 3 mM 4-AP (red trace) eliminated the slow component and resulted in $I_{gOFF}$ with a single fast component of 0.55 ± 0.02 ms ($n$ = 4). (D) Voltage- and time-dependent slowing in $I_{gOFF}$. To test whether the slow component in $I_{gOFF}$ is linked to the concerted step of opening, envelope protocols were used with depolarizations to −5 mV or +60 mV. At −5 mV, $I_{gOFF}$ decayed mono-exponentially with a $\tau_{OFF,fast}$ of 0.20 ± 0.02 ms ($n$ = 3). In contrast, depolarizations to +60 mV resulted in an $I_{gOFF}$ with two kinetic components. Very short steps generated an $I_{gOFF}$ that decayed mono-exponentially with a time component $\tau_{OFF,fast}$ of 0.51 ± 0.04 ms ($n$ = 6), whereas with longer steps, $I_{gOFF}$ decayed markedly slower, with a $\tau_{OFF,slow}$ of 3.44 ± 0.11 ms ($n$ = 6). The addition of 3 mM 4-AP abolished the time-dependent slowing of $I_{gOFF}$, resulting in a single fast component with a $\tau_{OFF,fast}$ of 0.58 ± 0.03 ms ($n$ = 3) independent of the step duration.

opening (Loboda and Armstrong, 2001). Application of 3 mM 4-AP, a concentration sufficient to fully inhibit Kv3.1 ionic current, resulted in a disappearance of the slow component of $I_{gOFF}$, whereas the fast kinetics remained unaltered ($\tau$ of 0.55 ± 0.02 ms, $n = 4$) irrespective of step duration (Fig. 2, C and D). This time constant is comparable to the $I_{gOFF,fast}$ decay in control conditions. Furthermore, 4-AP resulted in a 14.7 ± 1.0% ($n = 5$) reduction of the total charge movement, indicating that the amount of charge carried by the final concerted step in the activation pathway is somewhat larger in Kv3.1 than in *Shaker*, where it was reported to be ~5% (Loboda and Armstrong, 2001).

### Gambierol immobilizes the VSD in the resting state

We next investigated the effect of gambierol on the gating charge movement of Kv3.1 channels. Application of 100 nM gambierol resulted in a 96 ± 1% ($n = 4$) reduction of both $I_{gON}$ and $I_{gOFF}$ charge movement (Fig. 3, A and B) evoked by depolarizations to +40 mV. This loss in charge movement is substantially more than the 15% of gating charge linked to the final concerted step in channel opening; therefore, gambierol most likely prevents VSD movement between deeper closed states. The time course of reduction in total charge movement (Fig. 3 C) was determined by integrating $I_{gOFF}$ and occurred with a time constant of 100 ± 4 s ($n = 4$), which is clearly slower than the onset of ionic current inhibition. Because the opening of the gate occurs in a concerted manner, requiring all four VSDs being in the active state, then preventing one VSD from reaching its activated state would be sufficient to inhibit channel opening. Indeed, monitoring the kinetic behavior of $I_{gOFF}$ showed a clear decrease of $I_{gOFF,slow}$ in the overall $I_{gOFF}$ decay that developed quicker than the reduction of the total $Q_{OFF}$ charge movement. To quantify this, the amplitude of the $I_{gOFF,slow}$ was plotted as a function of gambierol application time (Fig. 3 D). $I_{gOFF,slow}$ disappeared with a time constant of 68 ± 3 s ($n = 4$), which was similar to the onset of ionic current inhibition. Furthermore, the decrease in $I_{gOFF,slow}$ was accompanied with an initial increase in the amplitude of $I_{gOFF,fast}$ (Fig. 3, B and E). This suggests that when one toxin has bound to one of the four binding sites, the concerted step of S6 gate opening cannot occur, precluding gate opening. The further reduction in $I_{gOFF,fast}$ amplitude then reflects progressive immobilization of all VSDs. Recovery of $I_{gOFF,slow}$ upon washout (Fig. 3 D) was extremely slow and displayed an initial lag phase, similar to the washout of the ionic current (Kopljar et al., 2009).

Determination of the QV curve in the presence of 300 nM gambierol (Fig. 4, A and B) was done by brief 50-ms pulses up to +160 mV, yielding a $V_{1/2}$ of 124 ± 6 mV

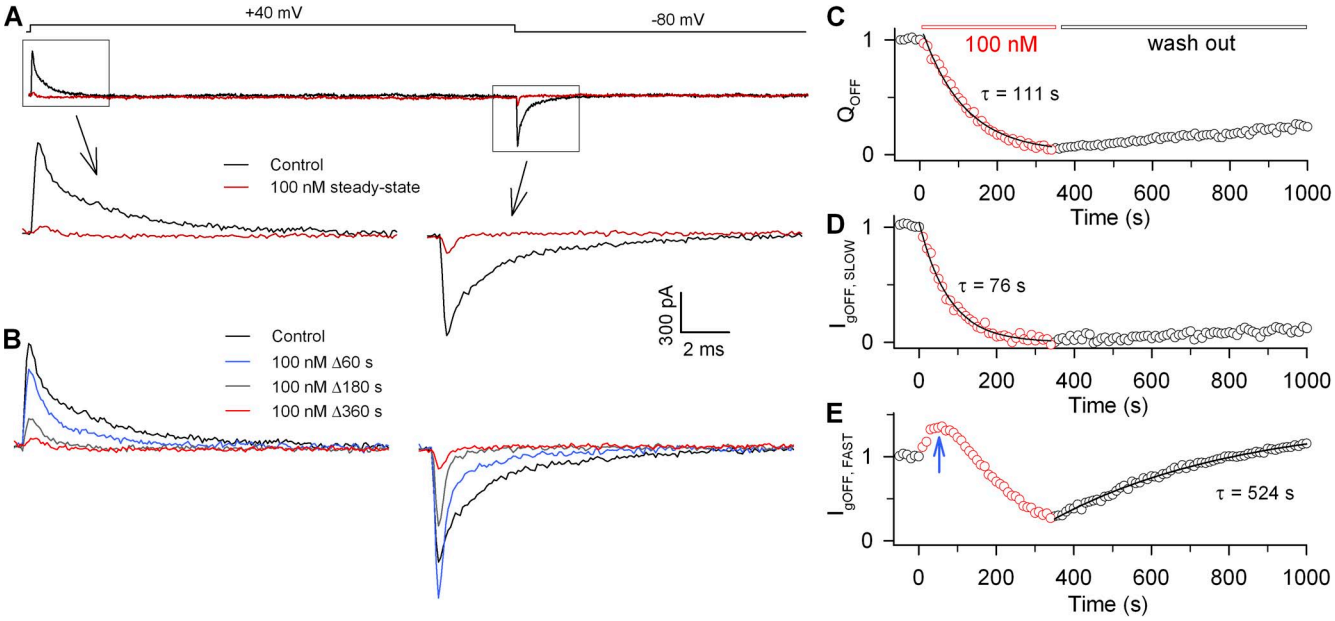


**Figure 3.** Gambierol immobilizes gating charge movement. (A) Gating current recordings in control (black) and after steady-state inhibition with 100 nM gambierol (red). $I_{gON}$ were elicited by 125-ms steps to +40 mV from −80 mV holding potential. Subsequently, $I_{gOFF}$ were recorded upon repolarizing back to −80 mV. (B) The development of gating current inhibition in A was monitored with steps every 10 s; for clarity, only the gating currents in control (black) and after 60 s (blue), 180 s (gray), and 360 s (red) of gambierol wash-in are shown. (C) Total $Q_{OFF}$ charge movement upon gambierol wash-in (red) and washout was obtained by integrating the $I_{gOFF}$ currents from B and plotted as a function of time. (D and E) Changes in the amplitude of the slow and fast component of $I_{gOFF}$. In D, the gradual decrease in $I_{gOFF,slow}$ was fitted with a mono-exponential function (solid line), yielding a time constant of 76 s. In E, the recovery of $I_{gOFF,fast}$ upon washout yielded a time constant of 524 s. Note the transient increase of $I_{gOFF,fast}$ (blue arrow) peaks around 60 s (blue tracing in B).

with a $k$ of 21 ± 2 mV for $I_{gOFF}$ ($n$ = 4). Hence, gambierol acts as a gating modifier that shifts the voltage dependence of charge movement by ∼120 mV toward more depolarized potentials. In control, the decay of $I_{gON}$ mirrors the rise in ionic current (Fig. 4 C), as has been shown in *Shaker* (Schoppa et al., 1992; Zagotta et al., 1994b). However, under influence of gambierol, the ionic current does not activate within the time window of $I_{gON}$ decay. Moreover, the maximal amount of charge moved (determined from the amplitude of the QV curve) was 81 ± 2% ($n$ = 4) of the total charge in control, which is comparable to the amount of charge moved under influence of 4-AP. These data suggest that gambierol-bound channels can move up to the activated-not-open state upon strong depolarizations; however, they cannot pass the concerted step leading to pore opening.

### A single toxin-binding site interaction inhibits ion permeation

The gating current data suggest that a single toxin-binding site interaction is sufficient to inhibit ion permeation,

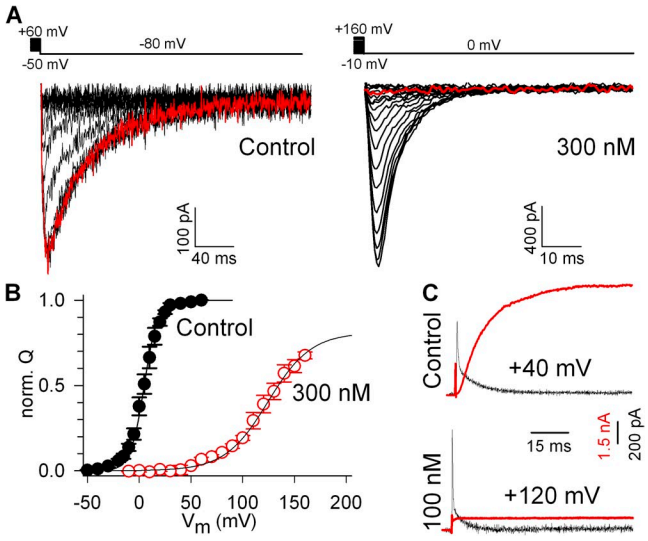


**Figure 4.** Gambierol shifts the voltage dependence of gating. (A) Kv3.1 gating current recordings in control (left) and after steady-state inhibition with 300 nM gambierol (right). $I_{gON}$ were elicited by 50-ms steps from −80 mV to potentials between −50 and +60 mV in control and between −10 and +160 mV in the presence of gambierol. Subsequently, $I_{gOFF}$ were recorded upon repolarization back to −80 mV in control or to 0 mV (due to shifted kinetics) in the presence of gambierol. For clarity, only the $I_{gOFF}$ tracings are shown. The red tracing represents $I_{gOFF}$ after a +40-mV depolarization. (B) Normalized QV relationships for $I_{gOFF}$. The $V_{1/2}$ of $Q_{OFF}$ in presence of 300 nM gambierol (+124 ± 6 mV; $n$ = 4) reflected an ∼120-mV depolarizing shift compared with the $V_{1/2}$ of $I_{gOFF}$ in control. (C) Superposition of scaled gating (black) and ionic currents (red). Currents in control (top) were elicited at +40 mV, and displayed similar kinetics for ionic activation and $I_{gON}$ decay. In the presence of 100 nM gambierol (bottom), no ionic current activation was observed in the time window of $I_{gON}$ decay (elicited at +120 mV).

whereas current recovery requires all binding sites to be toxin-free. To determine the effect of gambierol on a channel containing only a single high-affinity binding site, we created several Kv3.1 concatemers in which four subunits were linked together, resulting in a single polypeptide (Fig. S1 A). The WT concatemer yielded functional channels with biophysical properties and gambierol sensitivity ($IC_{50}$ of 1.2 ± 0.1 nM, $n$ = 3) similar to WT Kv3.1 channels, assembled from monomers (Figs. 5 A and S1). Mutation of the residue T427 in the S6 segment to a valine drastically reduced the channel's sensitivity for gambierol (Kopljar et al., 2009). In agreement, the concatemer with four T427V mutant subunits resulted in channels with a 1,000-fold lower affinity, yielding an $IC_{50}$ of 2.3 ± 0.3 µM ($n$ = 4), which was comparable to the affinity of tetramers assembled from T427V monomers. A concatemer that contains one WT and three T427V subunits would yield Kv3.1 channels with only a single high-affinity binding site. Two such concatemers with a different position of the WT subunit were created: WT-mut-mut-mut and mut-mut-WT-mut, which posses the high-affinity binding site in the first and third subunit, respectively. The mut-mut-WT-mut concatemer generated functional channels, with a concentration dependence of gambierol inhibition that could be fitted with a Hill equation yielding an $IC_{50}$ of 23 ± 3 nM and a Hill coefficient $n_H$ of 0.86 ± 0.09 ($n$ = 5; Fig. 5, A and B). The WT-mut-mut-mut concatemer had a similar $IC_{50}$ of 20 ± 2 nM ($n$ = 3), which indicates that the position of the WT subunit within the concatemer did not affect the affinity for gambierol.

The kinetics of gambierol binding and unbinding at a single high-affinity binding site were explored using the mut-mut-WT-mut concatemer (Fig. 5 D). Onset of current inhibition with 100 nM gambierol occurred with a time constant of 110 ± 8 s ($n$ = 3) or a rate λ of 0.009 $s^{-1}$, yielding an apparent association rate constant $k$ of 0.08 × $10^6$ $M^{-1}s^{-1}$. In contrast to WT Kv3.1 channels, the recovery from current inhibition upon gambierol washout developed mono-exponentially in the mut-mut-WT-mut concatemer with a time constant of 698 ± 78 s ($n$ = 4) or a dissociation rate constant $l$ of 1.4 × $10^{-3}$ $s^{-1}$ that was still relatively slow. The initial lag phase in the recovery from current inhibition observed in WT Kv3.1 channels (Fig. 5 C) upon washout of a saturating 100-nM gambierol concentration could be explained by having more than one binding site occupied. To compare the association and dissociation kinetics between the concatemer with a single high-affinity site and WT Kv3.1 channels under nonsaturating conditions, we used 40 nM for the mut-mut-WT-mut concatemer and 10 nM for the WT channel, each yielding ∼70% inhibition (Fig. 5, C and D). Under these conditions, the onset of inhibition was similar and the washout displayed a shorter lag phase for WT Kv3.1, followed by a mono-exponential component, equally

slow after exposure with 100 nM (Fig. 5 C). For the concatemer, the recovery after 40 nM followed a mono-exponential time course similar to that after 100 nM. If the toxin acts through the lipid bilayer, the slow dissociation could be caused by the departitioning of gambierol from the plasma membrane. If this would be the rate-limiting step during washout, then the washout in the low-affinity T427V mutant should be similarly slow. However, the T427V mutant displayed a relatively fast washout with a time constant of 21 ± 2 s ($n$ = 3; Fig. S2), indicating that the slow dissociation kinetics (Fig. 5, C and D) reflect the toxin–channel dissociation rate constants.

## DISCUSSION

Ladder-shaped polyether toxins (e.g., maitotoxin and yessotoxin) have been proposed to target transmembrane proteins within the lipid bilayer (Murata et al., 2008). Their unique structure, in which the spacing of the ether-oxygens closely matches the pitch of α-helices of transmembrane proteins, enables multiple interactions involving hydrogen bonding and/or hydrophobic interactions (Murata et al., 2008; Ujihara et al., 2008, 2010; Torikai et al., 2008). Hence, its amphipathic nature might allow gambierol to modulate Kv channels through the lipid bilayer, where the closed channel conformation represents the high-affinity binding site.

The analysis of the state-dependence of the affinity of Kv3.1 channels for gambierol showed that open channels could not be inhibited in the nanomolar range (Fig. 1 A). However, subsequent induction of current inhibition (Fig. 1 B) occurred with a τ of 36 s, which is almost twofold faster than the τ of 65 s determined immediately after gambierol application (Kopljar et al., 2009). If gambierol needs to partition in the membrane to induce channel inhibition, then the kinetics of current inhibition (τ of 65 s) immediately after gambierol application also include this lipid-partitioning step. In this scenario, the τ of 36 s most likely reflects the effective onset of channel inhibition for an apparent toxin concentration of 100 nM. Pushing gambierol-bound channels toward the open state (Fig. 1 C) by applying strong membrane depolarizations reverted the inhibition, indicating that activated channels have a much lower affinity than those residing in the resting (closed) state. Furthermore, the reinduction of inhibition developed with a τ of 39 s, which is similar to the effective onset of channel inhibition, suggesting that current recovery had originated from gambierol dissociation.

The effect of gambierol on gating currents, which reflect the movement of the VSDs, provided further insight into the mechanism of channel inhibition. In control, the $V_{1/2}$ of $Q_{ON}$ and $Q_{OFF}$ was ∼15 mV more

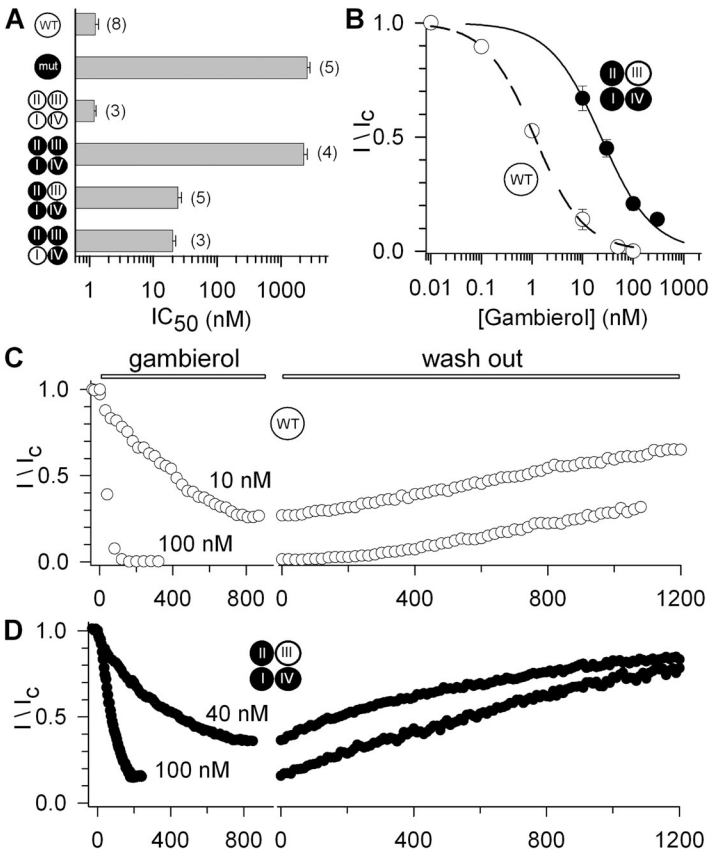


**Figure 5.** A single high-affinity binding site is sufficient for current inhibition. (A) Bar chart displaying the gambierol sensitivity ($IC_{50}$ values) for Kv3.1 channels assembled from WT or T427V monomers, and several concatemers with different WT and T247V subunit composition. The position of the subunits within the concatemer is numbered from I to IV. WT and mutant subunits are represented with white and black color coding, respectively. Error bars indicate SEM. (B) Concentration dependence of inhibition for WT Kv3.1 (open symbols, data taken from Kopljar et al., 2009) and the mut-mut-WT-mut concatemer (closed symbols) obtained from the normalized current suppression as a function of the gambierol concentration. (C and D) Time course of inhibition of WT Kv3.1 and the mut-mut-WT-mut concatemer by different gambierol concentrations, followed by a washout. Note the lag in the recovery for WT channels resulting in a sigmoidal time course. In contrast, the recovery in the concatemer occurred mono-exponentially.

negative than the $V_{1/2}$ of the voltage dependence of channel opening. Furthermore, with depolarizations >0 mV, there was a clear slowing in the decay of $I_{gOFF}$. Using envelope protocols, we provided evidence that this slowing in $I_{gOFF}$ is linked to the final concerted step leading to channel gate opening, as it is in other Kv channels (Bezanilla et al., 1994; Chen et al., 1997; Wang et al., 2007). This conclusion was further strengthened by the eliminated slow component in $I_{gOFF}$ by 4-AP, similar to the data for *Shaker* (Loboda and Armstrong, 2001). However, the fast component was left unaltered, indicating that this charge displacement is linked to VSD movements early in the activation pathway (before the concerted step) when the subunits move between the resting (closed) and the activated-not-open state.

Application of gambierol resulted in a time-dependent reduction of the total charge movement at +40 mV (for both $Q_{ON}$ and $Q_{OFF}$; Fig. 3, A and B). During this progressive loss of charge movement, the relative contribution of the fast ($I_{gOFF,fast}$) and slow ($I_{gOFF,slow}$) decaying component in $I_{gOFF}$ changed. The decrease in $I_{gOFF,slow}$ amplitude occurred on the same time scale as the onset of ionic current inhibition (Fig. 3 D), which indicated that inhibition of ion permeation is directly linked to the failure of channels to pass the final concerted opening step. The decrease in $I_{gOFF,slow}$ was initially accompanied by an increase in the amplitude of $I_{gOFF,fast}$ (but not of the total charge integral). Together with the data on the Kv3.1 concatemers that a single high-affinity binding site is sufficient for inhibition of the ionic current (Fig. 5), we interpret this as follows: when a single gambierol molecule binds to one of the four binding sites, this subunit cannot move to the activated state, and the channel cannot open (i.e., pass the concerted step); however, the other subunits, free of gambierol, are still able to move their VSD to the activated state from which $Q_{OFF}$ return is fast (resulting in the initial increase in amplitude of $I_{gOFF,fast}$). Subsequently, interaction of gambierol with the remaining binding sites results in a further progressive decrease in $I_{gON}$ and $I_{gOFF}$ amplitude until hardly any gating charge is moving when all four binding sites on the channel become occupied.

Whereas ionic current recovery at strong depolarizations was slow (Fig. 1 C), similar potentials elicited gating currents that were remarkably fast and allowed us to determine that gambierol (300 nM) caused a 120 mV depolarized shift in the voltage dependence of charge movement (Fig. 4, A and B). Under these conditions, 81% of the total charge moved, which is similar to the 85% that moved in the presence of 4-AP. This suggests that the recorded gating currents represent VSD movements between the resting and the activated-not-open state. Furthermore, ionic currents in presence of gambierol did not display channel activation within the time window of $I_{gON}$ movement (Fig. 4 C), which is consistent with the proposal that gambierol-bound subunits can move their VSD up to the activated state upon strong depolarizations, but cannot pass the concerted step leading to channel opening as long as gambierol remained bound.

Kv3.1 concatemers with a single WT binding site displayed an $IC_{50}$ of 20 nM, which should represent the intrinsic affinity of a single binding site. Indeed, assuming four equivalent and independent binding sites, this would yield an apparent $IC_{50}$ of 3–4 nM for the WT channel, which is close to the reported $IC_{50}$ of 1.2 nM (Kopljar et al., 2009). Onset of gambierol inhibition was about twofold slower ($\tau$ = 110 s) than previously reported for WT (Kopljar et al., 2009). This differs from the fourfold change expected in the case of four independent binding sites per channel. However, the value of ~65 s for WT may not reflect the true toxin–channel interaction kinetics: as argued before, a value of 35–40 s is more likely. Under nonsaturating conditions, a fourfold higher gambierol concentration was indeed required to obtain a similar time course of inhibition in the mut-mut-WT-mut concatemer compared with WT channels (40 nM compared with 10 nM, respectively; Fig. 5, C and D). The washout in the mut-mut-WT-mut concatemer was mono-exponential ($\tau$ = 698 s) and faster compared with WT channels. The association and dissociation rate constants $k$ and $l$ obtained from this concatemer most likely reflect the intrinsic kinetics for the interaction of gambierol with the resting (closed) state. Indeed, in WT channels, the dissociation kinetics are complicated by the fourfold symmetry (Kopljar et al., 2009). Thus, the washout in WT channels displays a more complex time course with an initial lag phase, whereas the washout in the mut-mut-WT-mut concatemer (Fig. 5 D) was mono-exponential and similar to the recovery of $I_{gOFF,fast}$ (Fig. 3 E). These data suggest that a single toxin-binding site interaction is sufficient to inhibit ion permeation, whereas current recovery requires all binding sites to be toxin-free.

Several tarantula and sea anemone toxins (e.g., hanatoxin, BDS-II) are well-known gating modifiers of Kv channels (Swartz, 2007; Wang et al., 2007). Both peptide toxins also stabilize the resting state, but their mechanism differs from the polyether toxin gambierol. Hanatoxin and BDS-II act as a cargo attached to the VSD imposing an energetic penalty for its movement (Phillips et al., 2005; Wang et al., 2007), thus requiring stronger depolarizations to open these toxin-bound channels. In contrast, gambierol acts like an anchor that immobilizes the gating machinery in a more profound manner. Although hanatoxin-bound channels can open, gambierol-bound ones cannot and require dissociation of the toxin to restore permeation.

Based on the experimental data, we propose two mechanisms for channel inhibition by gambierol, both resulting in VSD immobilization. For *Shaker*-type Kv channels, it has been proposed that the VSD has to

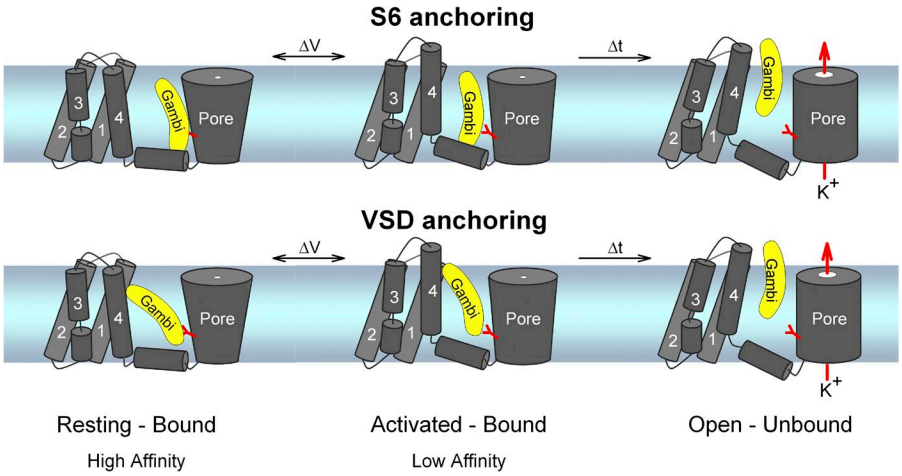


**Figure 6.** Cartoon of the proposed mechanistic models (S6 gate and VSD anchoring) for Kv channel inhibition. Residue T427 in S6 is shown in red, and for clarity only one VSD is shown. The closed channel conformation with the VSD in the resting state forms the high-affinity state that is stabilized by gambierol (resting-bound). With strong depolarizations (ΔV), the VSDs move to the activated state, which displays a lower affinity for gambierol (activated-bound). Spending sufficient time (Δt) in this low-affinity conformation results in an accelerated unbinding of gambierol, allowing channels to open (open-unbound).

perform work to open the S6 activation gate (Yifrach and MacKinnon, 2002; Jensen et al., 2012); i.e., the S6 gate impedes the VSD from moving. Furthermore, it has been shown that VSD transitions from the resting to the activated state already induce rearrangements of the intracellular S6 gate region; i.e., before the concerted opening step (del Camino et al., 2005). Because the gambierol binding site involves residues of the S5 and S6 segment, a possible mechanistic explanation for channel inhibition is that gambierol prevents these early pre-open S6 movements (that are tied directly to the VSD), causing a much stronger stabilization of the resting state ($\Delta\Delta G_o$ = 2.71 kcal/mol). Hence, much larger depolarizations are required to move the VSDs to the activated state, but this will not result in ion permeation as long as gambierol is bound at one of the four equivalent binding sites (Fig. 6, first model). At this point, gambierol isolates the final concerted step of S6 gate opening from earlier VSD movements, as observed for 4-AP or mutations in the S4 segment and S4–S5 linker (McCormack et al., 1991; Schoppa and Sigworth, 1998; Ledwell and Aldrich, 1999). In contrast to the effects from gambierol, the gating currents originating from pre-open VSD movements were almost normal in these channel mutants or after 4-AP block, indicating that the early S6 motions (linked to these pre-open VSD movements) were still freely allowed. An alternative mechanistic explanation for channel inhibition (Fig. 6, second model) would be that gambierol interacts directly with a VSD and anchors it to the pore domain (possibly through the residue T427). The movement of the VSDs to their activated state would then alter the conformation of the binding site, leading to a decreased affinity. In either model, occupancy of one of the four gambierol binding sites immobilizes a single VSD. Unfortunately, the expression level of the concatemeric constructs was too low to test this hypothesis directly with gating current analysis. Consequently, we cannot exclude the possibility that one gambierol molecule affects multiple (i.e., two) VSDs. However, the time dependence of the reduction of total charge and $I_{gOFF,fast}$ was noticeable different from the reduction of the $I_{gOFF,slow}$ component. This indicates that one gambierol molecule cannot affect all four VSDs simultaneously, because in that case both processes should occur simultaneously. The initial lag in the time course of recovery and the difference in the apparent affinities of WT and mut-mut-WT-mut concatemers is also most easily explained by a model with four independent binding sites.

Thus, we provide a novel mechanism for Kv channel inhibition that relies on anchoring the gating machinery in its resting (closed) state. Upon strong depolarizations, the VSD can be pushed toward its activated-not-open state, but as long as gambierol is bound, the channel gate remains closed, similar to the effect of 4-AP or channel mutations that isolate the final concerted step of channel opening. The conformational change associated with this activated-not-open state most likely reduces the affinity for gambierol and presumably enhances the dissociation rate. Consequently, the channel eventually opens when fully freed of toxin (Fig. 6). However, the depolarizations required for activating gambierol-bound channels exceed by far the physiologically relevant voltage range.

I. Kopljar is a fellow with the Vlaams Instituut voor de bevordering van het Wetenschappelijk-Technologisch Onderzoek in de Industrie (IWT). This work was supported by the Interuniversity Attraction Poles (IAP) program P6/31 of the Belgian Federal Science Policy Office, grants from Fonds voor Wetenschappelijk Onderzoek Vlaanderen (FWO; G.0449.11 to D.J. Snyders and G.0433.12 to D.J. Snyders and J. Tytgat), and grant GM56677 from the National Institutes of Health, General Medical Sciences (to J.D. Rainier).

Kenton J. Swartz served as editor.

Submitted: 28 August 2012
Accepted: 16 January 2013

## REFERENCES


Bezanilla, F. 2008. How membrane proteins sense voltage. *Nat. Rev. Mol. Cell Biol.* 9:323–332. http://dx.doi.org/10.1038/nrm2376

Bezanilla, F., E. Perozo, and E. Stefani. 1994. Gating of *Shaker* $K^+$ channels: II. The components of gating currents and a model of channel activation. *Biophys. J.* 66:1011–1021. http://dx.doi.org/10.1016/S0006-3495(94)80882-3

Birinyi-Strachan, L.C., S.J. Gunning, R.J. Lewis, and G.M. Nicholson. 2005. Block of voltage-gated potassium channels by Pacific ciguatoxin-1 contributes to increased neuronal excitability in rat sensory neurons. *Toxicol. Appl. Pharmacol.* 204:175–186. http://dx.doi.org/10.1016/j.taap.2004.08.020

Blunck, R., and Z. Batulan. 2012. Mechanism of electromechanical coupling in voltage-gated potassium channels. *Front Pharmacol.* 3:166. http://dx.doi.org/10.3389/fphar.2012.00166

Catterall, W.A., S. Cestèle, V. Yarov-Yarovoy, F.H. Yu, K. Konoki, and T. Scheuer. 2007. Voltage-gated ion channels and gating modifier toxins. *Toxicon.* 49:124–141. http://dx.doi.org/10.1016/j.toxicon.2006.09.022

Chen, F.S., D. Steele, and D. Fedida. 1997. Allosteric effects of permeating cations on gating currents during $K^+$ channel deactivation. *J. Gen. Physiol.* 110:87–100. http://dx.doi.org/10.1085/jgp.110.2.87

Cuypers, E., Y. Abdel-Mottaleb, I. Kopljar, J.D. Rainier, A.L. Raes, D.J. Snyders, and J. Tytgat. 2008. Gambierol, a toxin produced by the dinoflagellate *Gambierdiscus toxicus*, is a potent blocker of voltage-gated potassium channels. *Toxicon.* 51:974–983. http://dx.doi.org/10.1016/j.toxicon.2008.01.004

del Camino, D., M. Kanevsky, and G. Yellen. 2005. Status of the intracellular gate in the activated-not-open state of *shaker* $K^+$ channels. *J. Gen. Physiol.* 126:419–428. http://dx.doi.org/10.1085/jgp.200509385

Ghiaroni, V., M. Sasaki, H. Fuwa, G.P. Rossini, G. Scalera, T. Yasumoto, P. Pietra, and A. Bigiani. 2005. Inhibition of voltage-gated potassium currents by gambierol in mouse taste cells. *Toxicol. Sci.* 85:657–665. http://dx.doi.org/10.1093/toxsci/kfi097

Grissmer, S., A.N. Nguyen, J. Aiyar, D.C. Hanson, R.J. Mather, G.A. Gutman, M.J. Karmilowicz, D.D. Auperin, and K.G. Chandy. 1994. Pharmacological characterization of five cloned voltage-gated $K^+$ channels, types Kv1.1, 1.2, 1.3, 1.5, and 3.1, stably expressed in mammalian cell lines. *Mol. Pharmacol.* 45:1227–1234.

Hidalgo, J., J.L. Liberona, J. Molgó, and E. Jaimovich. 2002. Pacific ciguatoxin-1b effect over $Na^+$ and $K^+$ currents, inositol 1,4,5-triphosphate content and intracellular $Ca^{2+}$ signals in cultured rat myotubes. *Br. J. Pharmacol.* 137:1055–1062. http://dx.doi.org/10.1038/sj.bjp.0704980

Jensen, M.O., V. Jogini, D.W. Borhani, A.E. Leffler, R.O. Dror, and D.E. Shaw. 2012. Mechanism of voltage gating in potassium channels. *Science.* 336:229–233. http://dx.doi.org/10.1126/science.1216533

Johnson, H.W., U. Majumder, and J.D. Rainier. 2006. Total synthesis of gambierol: subunit coupling and completion. *Chemistry.* 12:1747–1753. http://dx.doi.org/10.1002/chem.200500994

Kopljar, I., A.J. Labro, E. Cuypers, H.W. Johnson, J.D. Rainier, J. Tytgat, and D.J. Snyders. 2009. A polyether biotoxin binding site on the lipid-exposed face of the pore domain of Kv channels revealed by the marine toxin gambierol. *Proc. Natl. Acad. Sci. USA.* 106:9896–9901. http://dx.doi.org/10.1073/pnas.0812471106

Labro, A.J., and D.J. Snyders. 2012. Being flexible: the voltage-controllable activation gate of kv channels. *Front Pharmacol.* 3:168. http://dx.doi.org/10.3389/fphar.2012.00168

Ledwell, J.L., and R.W. Aldrich. 1999. Mutations in the S4 region isolate the final voltage-dependent cooperative step in potassium channel activation. *J. Gen. Physiol.* 113:389–414. http://dx.doi.org/10.1085/jgp.113.3.389

Li-Smerin, Y., D.H. Hackos, and K.J. Swartz. 2000. A localized interaction surface for voltage-sensing domains on the pore domain of a $K^+$ channel. *Neuron.* 25:411–423. http://dx.doi.org/10.1016/S0896-6273(00)80904-6

Loboda, A., and C.M. Armstrong. 2001. Resolving the gating charge movement associated with late transitions in K channel activation. *Biophys. J.* 81:905–916. http://dx.doi.org/10.1016/S0006-3495(01)75750-5

Long, S.B., E.B. Campbell, and R. Mackinnon. 2005. Crystal structure of a mammalian voltage-dependent *Shaker* family $K^+$ channel. *Science.* 309:897–903. http://dx.doi.org/10.1126/science.1116269

Lu, Z., A.M. Klem, and Y. Ramu. 2002. Coupling between voltage sensors and activation gate in voltage-gated $K^+$ channels. *J. Gen. Physiol.* 120:663–676. http://dx.doi.org/10.1085/jgp.20028696

Mattei, C., M. Marquais, S. Schlumberger, J. Molgó, J.P. Vernoux, R.J. Lewis, and E. Benoit. 2010. Analysis of Caribbean ciguatoxin-1 effects on frog myelinated axons and the neuromuscular junction. *Toxicon.* 56:759–767. http://dx.doi.org/10.1016/j.toxicon.2009.07.026

McCormack, K., M.A. Tanouye, L.E. Iverson, J.W. Lin, M. Ramaswami, T. McCormack, J.T. Campanelli, M.K. Mathew, and B. Rudy. 1991. A role for hydrophobic residues in the voltage-dependent gating of *Shaker* $K^+$ channels. *Proc. Natl. Acad. Sci. USA.* 88:2931–2935. http://dx.doi.org/10.1073/pnas.88.7.2931

Murata, M., N. Matsumori, K. Konoki, and T. Oishi. 2008. Structural features of dinoflagellate toxins underlying biological activity as viewed by NMR. *Bull. Chem. Soc. Jpn.* 81:307–319. http://dx.doi.org/10.1246/bcsj.81.307

Nicholson, G.M., and R.J. Lewis. 2006. Ciguatoxins: Cyclic polyether modulators of voltage-gated ion channel function. *Mar. Drugs.* 4:82–118. http://dx.doi.org/10.3390/md403082

Perozo, E., D.M. Papazian, E. Stefani, and F. Bezanilla. 1992. Gating currents in Shaker K+ channels. Implications for activation and inactivation models. *Biophys. J.* 62:160–171. http://dx.doi.org/10.1016/S0006-3495(92)81802-7

Phillips, L.R., M. Milescu, Y. Li-Smerin, J.A. Mindell, J.I. Kim, and K.J. Swartz. 2005. Voltage-sensor activation with a tarantula toxin as cargo. *Nature.* 436:857–860. http://dx.doi.org/10.1038/nature03873

Satake, M., M. Murata, and T. Yasumoto. 1993. Gambierol: a new toxic polyether compound isolated from the marine dinoflagellate *Gambierdiscus toxicus*. *J. Am. Chem. Soc.* 115:361–362. http://dx.doi.org/10.1021/ja00054a061

Schlumberger, S., C. Mattei, J. Molgó, and E. Benoit. 2010a. Dual action of a dinoflagellate-derived precursor of Pacific ciguatoxins (P-CTX-4B) on voltage-dependent $K(^+)$ and $Na(^+)$ channels of single myelinated axons. *Toxicon.* 56:768–775. http://dx.doi.org/10.1016/j.toxicon.2009.06.035

Schlumberger, S., G. Ouanounou, E. Girard, M. Sasaki, H. Fuwa, M.C. Louzao, L.M. Botana, E. Benoit, and J. Molgó. 2010b. The marine polyether gambierol enhances muscle contraction and blocks a transient $K(^+)$ current in skeletal muscle cells. *Toxicon.* 56:785–791. http://dx.doi.org/10.1016/j.toxicon.2010.06.001

Schoppa, N.E., and F.J. Sigworth. 1998. Activation of Shaker potassium channels. III. An activation gating model for wild-type and V2 mutant channels. *J. Gen. Physiol.* 111:313–342. http://dx.doi.org/10.1085/jgp.111.2.313

Schoppa, N.E., K. McCormack, M.A. Tanouye, and F.J. Sigworth. 1992. The size of gating charge in wild-type and mutant Shaker potassium channels. *Science.* 255:1712–1715. http://dx.doi.org/10.1126/science.1553560

Shieh, C.C., K.G. Klemic, and G.E. Kirsch. 1997. Role of transmembrane segment S5 on gating of voltage-dependent $K^+$

channels. *J. Gen. Physiol.* 109:767–778. http://dx.doi.org/10.1085/jgp.109.6.767

Stefani, E., L. Toro, E. Perozo, and F. Bezanilla. 1994. Gating of *Shaker* $K^+$ channels: I. Ionic and gating currents. *Biophys. J.* 66:996–1010. http://dx.doi.org/10.1016/S0006-3495(94)80881-1

Swartz, K.J. 2007. Tarantula toxins interacting with voltage sensors in potassium channels. *Toxicon.* 49:213–230. http://dx.doi.org/10.1016/j.toxicon.2006.09.024

Swartz, K.J., and R. MacKinnon. 1997. Hanatoxin modifies the gating of a voltage-dependent $K^+$ channel through multiple binding sites. *Neuron.* 18:665–673. http://dx.doi.org/10.1016/S0896-6273(00)80306-2

Torikai, K., T. Oishi, S. Ujihara, N. Matsumori, K. Konoki, M. Murata, and S. Aimoto. 2008. Design and synthesis of ladder-shaped tetracyclic, heptacyclic, and decacyclic ethers and evaluation of the interaction with transmembrane proteins. *J. Am. Chem. Soc.* 130:10217–10226. http://dx.doi.org/10.1021/ja801576v

Ujihara, S., T. Oishi, K. Torikai, K. Konoki, N. Matsumori, M. Murata, Y. Oshima, and S. Aimoto. 2008. Interaction of ladder-shaped polyethers with transmembrane alpha-helix of glycophorin A as evidenced by saturation transfer difference NMR and surface plasmon resonance. *Bioorg. Med. Chem. Lett.* 18:6115–6118. http://dx.doi.org/10.1016/j.bmcl.2008.10.020

Ujihara, S., T. Oishi, R. Mouri, R. Tamate, K. Konoki, N. Matsumori, M. Murata, Y. Oshima, N. Sugiyama, M. Tomita, and Y. Ishihama. 2010. Detection of Rap1A as a yessotoxin binding protein from blood cell membranes. *Bioorg. Med. Chem. Lett.* 20:6443–6446. http://dx.doi.org/10.1016/j.bmcl.2010.09.080

Wang, Z., B. Robertson, and D. Fedida. 2007. Gating currents from a Kv3 subfamily potassium channel: charge movement and modification by BDS-II toxin. *J. Physiol.* 584:755–767. http://dx.doi.org/10.1113/jphysiol.2007.140145

Yifrach, O., and R. MacKinnon. 2002. Energetics of pore opening in a voltage-gated $K(^+)$ channel. *Cell.* 111:231–239. http://dx.doi.org/10.1016/S0092-8674(02)01013-9

Zagotta, W.N., T. Hoshi, and R.W. Aldrich. 1994a. *Shaker* potassium channel gating. III: Evaluation of kinetic models for activation. *J. Gen. Physiol.* 103:321–362. http://dx.doi.org/10.1085/jgp.103.2.321

Zagotta, W.N., T. Hoshi, J. Dittman, and R.W. Aldrich. 1994b. *Shaker* potassium channel gating. II: Transitions in the activation pathway. *J. Gen. Physiol.* 103:279–319. http://dx.doi.org/10.1085/jgp.103.2.279